Earthq Eng & Eng Vib (2015) 14: 37-54 **DOI**: 10.1007/s11803-015-0005-6

Optimal vector-valued intensity measure for seismic collapse assessment of structures

Masood Yakhchalian[1†], Ahmad Nicknam[1‡] and Gholamreza Ghodrati Amiri[2§]

1. *School of Civil Engineering, Iran University of Science & Technology, Tehran, Iran*
2. *Center of Excellence for Fundamental Studies in Structural Engineering, School of Civil Engineering, Iran University of Science & Technology, Tehran, Iran*

Abstract: The present study is aimed to investigate the ability of different intensity measures (IMs), including response spectral acceleration at the fundamental period of the structure, $S_a(T_1)$, as a common scalar IM and twelve vector-valued IMs for seismic collapse assessment of structures. The vector-valued IMs consist of two components, with $S_a(T_1)$ as the first component and different parameters that are ratios of scalar IMs, as well as the spectral shape proxies ε_{Sa} and N_p, as the second component. After investigating the properties of an optimal IM, a new vector-valued IM that includes the ratio of $S_a(T_1)$ to the displacement spectrum intensity (DSI) as the second component is proposed. The new IM is more efficient than other IMs for predicting the collapse capacity of structures. It is also sufficient with respect to magnitude, source-to-site distance, and scale factor for collapse capacity prediction of structures. To satisfy the predictability criterion, a ground motion prediction equation (GMPE) is determined for $S_a(T_1)$/DSI by using the existing GMPEs. Furthermore, an empirical equation is proposed for obtaining the correlation between the components of the proposed IM. The results of this study show that using the new vector-valued IM leads to a more reliable seismic collapse assessment of structures.

Keywords: intensity measure; efficiency; sufficiency; displacement spectrum intensity; collapse capacity; fragility surface

1 Introduction

Nonlinear dynamic analysis is one of the methods for evaluating the demands on structures under earthquake excitations. When using this method for seismic performance assessment, it is necessary to investigate the properties of ground motions that are strongly related to the structural response. A parameter that describes the strength of a ground motion and quantifies its effect on structures is called intensity measure (IM). In seismic performance assessment of structures, IMs link the ground motion hazard with the structural response; therefore, using an appropriate IM plays an important role in the prediction of structural response or capacity. Studies continue to classify the existing IMs, and to propose new optimal IMs (e.g., Baker and Cornell, 2005; Bojórquez and Iervolino, 2010 and 2011; Bojórquez *et al.*, 2012; Tsantaki and Adam, 2013). In the performance-based earthquake engineering (PBEE) framework, the properties of an optimal IM are as follows: efficiency, that is, the ability of an IM to predict the response or capacity of a structure subjected to ground motion records with small dispersion; sufficiency, which is the ability of an IM to render the structural response or capacity conditionally independent of ground motion characteristics other than the IM; scaling robustness, which represents sufficiency with respect to scale factor when the records are linearly scaled to perform structural analyses; and predictability, that is, having a reliable ground motion prediction equation (GMPE) (Bradley *et al.*, 2010).

In the past, time-domain peak parameters, such as peak ground acceleration (PGA), peak ground velocity (PGV), and peak ground displacement (PGD), were common as scalar IMs. Currently, the elastic spectral acceleration at the fundamental period of the structure, $S_a(T_1)$, is the most common scalar IM. In recent researches on increasing the efficiency and sufficiency of IMs, vector-valued IMs have been proposed (e.g., Baker, 2005; Vamvatsikos and Cornell, 2005; Bojórquez and Iervolino, 2011), which mostly include two parameters but may have more. The reason for the increased

Correspondence to: Gholamreza Ghodrati Amiri, Center of Excellence for Fundamental Studies in Structural Engineering, School of Civil Engineering, Iran University of Science & Technology, P.O. Box 16765-163, Narmak, Tehran, Iran
Tel: +98 21 7724-0090; Fax: +98 21 7724-0398
E-mail: ghodrati@iust.ac.ir
†Ph.D. Candidate; ‡Assistant Professor; §Professor
Received August 15, 2013; **Accepted** March 25, 2014

efficiency and sufficiency of these IMs in comparison with scalar IMs is that a scalar IM represents a significant simplification of a ground motion. Vector-valued IMs contain more information about the ground motions; thus, their use may be more desirable for assessing the severity of a ground motion. Gehl *et al*. (2013) showed that some parameters that have little effect on the structural response when considered alone as an IM can have better performance when combined with a second IM in a vector-valued IM. The most common vector-valued IMs include $S_a(T_1)$ as the first component and spectral shape proxies, which imply the shape of the elastic response spectrum of a ground motion, as the second component. Two well-known spectral shape proxies are ε_{Sa} (Baker, 2005; Baker and Cornell, 2005) and N_P, as proposed by Bojórquez and Iervolino (2011).

Severe earthquakes may cause the collapse of structures and therefore can result in considerable loss of life (e.g., Sezen *et al*., 2000; Wang, 2008). Collapse prevention of structures has been the most important objective of building codes since their establishment. In the past, due to lack of proper analytical tools, quantitative assessment of structural collapse risk was impractical. Nowadays, with advances in PBEE and analytical tools, quantitative assessment of collapse risk of structures is becoming increasingly attractive (Eads *et al*., 2013). Collapse capacity prediction of a structure is one of the key steps in assessing its collapse risk. For more information about the analytical methods that are currently available to assess the seismic collapse capacity of building structures, the reader is referred to the comprehensive literature review carried out by Villaverde (2007).

The present study is aimed to investigate the efficiency and sufficiency of vector-valued IMs for collapse capacity prediction of structures. The idea of adding the ratio of two scalar IMs as the second component to $S_a(T_1)$ is applied to develop new vector-valued IMs. Additionally, the vectors ($S_a(T_1)$, ε_{Sa}) and ($S_a(T_1)$, N_P) are also considered as well-known vector-valued IMs. After investigating the desirable features of an optimal IM described above, an optimal vector-valued IM, ($S_a(T_1)$, $S_a(T_1)$/DSI), is proposed for seismic collapse assessment of structures. Displacement spectrum intensity (DSI) is a scalar IM that captures the severity of the long-period content of ground motions (Bradley, 2011a). To satisfy the predictability criterion for the proposed vector-valued IM, a GMPE is determined for its second component by using the existing GMPEs. Furthermore, the probabilistic characterization of a ground motion with the use of vector-valued IMs must account for the fact that the individual components of a vector-valued IM may be correlated. Therefore, to be able to use the new IM in vector-valued probabilistic seismic hazard analysis (VPSHA) (Bazzurro and Cornell, 2002), an empirical equation is proposed for calculating the correlation between its components.

2 Intensity measures

2.1 Well-known vector-valued intensity measures

Recently, some advanced vector-valued IMs have been proposed to overcome the shortcomings of traditional IMs. Baker (2005) proposed the epsilon value of a ground motion at the fundamental period of the structure (ε_{Sa}) as a spectral shape indicator. The parameter ε_{Sa} is defined as:

$$\varepsilon_{Sa} = \frac{\ln S_a(T_1) - \mu_{\ln Sa}}{\sigma_{\ln Sa}} \tag{1}$$

where $\ln S_a(T_1)$ is the natural logarithm of $S_a(T_1)$ in a particular ground motion; $\mu_{\ln Sa}$ and $\sigma_{\ln Sa}$ are the predicted mean and standard deviation of $\ln S_a(T_1)$, respectively. Thus, the parameter ε_{Sa} is the number of standard deviations by which the observed $\ln S_a(T_1)$ differs from the predicted mean. Baker (2005) found that the response of a structure to an earthquake is correlated with ε_{Sa}, and the collapse capacity of the structure increases with increasing ε_{Sa} of ground motion records used for collapse simulations. Other researchers (e.g., Haselton and Baker, 2006; Zareian, 2006; Goulet *et al*., 2007; Haselton *et al*., 2011) also investigated the effect of ε_{Sa} on the collapse capacity of structures. Due to the key effect of ε_{Sa} on the dynamic response of structures, Baker and Cornell (2005) proposed ($S_a(T_1)$, ε_{Sa}) as a vector-valued IM; thus, the effect of ε_{Sa} on the structural response can be accounted for by using this IM.

Another advanced vector-valued IM is ($S_a(T_1)$, N_P), which was proposed by Bojórquez and Iervolino (2011) as a spectral-shape-based IM. The parameter N_P is defined as:

$$N_P = \frac{S_{a_{\text{avg}}}(T_1 \ldots T_N)}{S_a(T_1)} \tag{2}$$

where $S_{a_{\text{avg}}}$ $(T_1 \ldots T_N)$ is the geometric mean of spectral accelerations over the period range of T_1–T_N ($T_N = 2T_1$). In fact, N_P is the average (geometric mean) of spectral accelerations over the specified period range normalized by $S_a(T_1)$. Based on the results of the study performed by Bojórquez and Iervolino (2011), the vector ($S_a(T_1)$, N_P) is more efficient than ($S_a(T_1)$, ε_{Sa}) for predicting the nonlinear response of structures.

2.2 Considered intensity measures

In this study, in addition to $S_a(T_1)$ as a common scalar IM and the well-known vector-valued IMs mentioned in Section 2.1, ten other vector-valued IMs are considered. These IMs include two components, with $S_a(T_1)$ as the first component (IM_1) and the ratios of different scalar IMs as the second component (IM_2). The scalar IMs that their ratios were used as the second component of the ten vector-valued IMs are as follows: $S_a(T_1)$, displacement spectrum intensity (DSI), spectrum intensity (SI), acceleration spectrum intensity (ASI), the peak IMs (i.e., PGA, PGV, and PGD), and Arias intensity (AI).

DSI, SI, and ASI are the integrals of the 5% damped displacement, pseudo-velocity, and pseudo-acceleration response spectra, over the period ranges presented in Table 1, respectively. These integral-based IMs, that is, DSI, SI, and ASI, indicate the severity of the long-, moderate-, and short-period content of ground motions, respectively. Therefore, they can be used as proxies for long-, moderate-, and short-period ground motion amplitudes. AI is an instrumental IM that can incorporate the cumulative effects of ground motion duration and intensity on the structural response. In fact, it represents the energy content of ground motions. Table 1 presents a summary of the definitions of AI and the aforementioned integral-based IMs.

GMPEs for DSI, SI, and ASI can be obtained from the GMPEs for spectral acceleration (Bradley *et al.*, 2009b; Bradley, 2010a, 2011a). Additionally, the technical literature includes some GMPEs for predicting AI (e.g., Campbell and Bozorgnia, 2012). Therefore, in choosing these IMs, their predictability was considered. Table 1 shows the vector-valued IMs considered in this study; it should be noted that all of these vector-valued IMs have unscalable IM_2 parameters. For instance, in the vector ($S_a(T_1)$, $S_a(T_1)^2$/AI), the term $S_a(T_1)^2$ was used as the numerator of the second component to make it unscalable.

3 The structures, ground motions, and method used for analyses

To investigate the ability of the considered IMs for seismic collapse assessment of structures, five reinforced concrete special moment resisting frames designed by Haselton and Deierlein (2008) were used. Table 2 presents the design ID numbers and fundamental periods of the structures. As mentioned by Haselton and Deierlein (2008), the fundamental periods of these structures are higher than some may expect, especially for low-rise buildings. This partially comes from the element stiffness model (Haselton *et al.*, 2008), which includes the effects of cracking, shear deformations, and bond-slip; this model is calibrated to represent the secant stiffness of an element at 40% of yielding. These longer periods also partially come from the fact that the stiffness of nonstructural components is neglected. The structural models were created with the OpenSees software (2006).

To analyze the structures, 67 ground motion records with a minimum usable frequency less than 0.2 Hz were extracted from the ground motion set used by Haselton and Deierlein (2008), which contains 78 ground motion records. The selected ground motion set consists of strong motions that may cause the structural collapse of modern buildings. The ground motion records were taken from the PEER NGA database (2008). The Campbell and Bozorgnia (2007) GMPE was used for the calculation of ε_{Sa} values. This GMPE was developed as part of the Next Generation Attenuation of Ground Motions (NGA) project. The NGA models are considerably more complicated than previous GMPEs and require several more input parameters. The framework proposed by Kaklamanos *et al.* (2011) was applied for estimating the unknown parameters required for the GMPE.

One of the methods for seismic performance assessment of structures by using a vector-valued IM, (IM_1, IM_2), is to perform incremental dynamic analysis

Table 1 Scalar and vector-valued IMs considered in this study

Considered IMs			Definition	Developer	Indicator of
IM No.	IM	Type			
1	$S_a(T_1)$	Scalar	$\mathrm{DSI}=\int_2^5 S_d(T,5\%)\mathrm{d}T$	Bradley (2011a)	Long-period severity
2	($S_a(T_1)$, $S_a(T_1)$/DSI)	Vector			
3	($S_a(T_1)$, $S_a(T_1)$/SI)	Vector	$\mathrm{SI}=\int_{0.1}^{2.5} S_v(T,5\%)\mathrm{d}T$	Housner (1952, 1963)	Moderate-period severity
4	($S_a(T_1)$, $S_a(T_1)$/ASI)	Vector			
5	($S_a(T_1)$, N_p)	Vector	$\mathrm{ASI}=\int_{0.1}^{0.5} S_a(T,5\%)\mathrm{d}T$	Von Thun *et al.* (1988)	Short-period severity
6	($S_a(T_1)$, ε_{Sa})	Vector			
7	($S_a(T_1)$, $S_a(T_1)$/PGA)	Vector	$\mathrm{AI}=\dfrac{\pi}{2g}\int_0^{t_{\max}} a(t)^2\mathrm{d}t$	Arias (1970)	Energy content
8	($S_a(T_1)$, $S_a(T_1)$/PGV)	Vector			
9	($S_a(T_1)$, $S_a(T_1)$/PGD)	Vector	ε_{Sa}(Eq. (1))	Baker (2005)	Spectral shape
10	($S_a(T_1)$, PGA/PGV)	Vector			
11	($S_a(T_1)$, PGA/PGD)	Vector	N_p(Eq. (2))	Bojórquez and Iervolino (2011)	Spectral shape
12	($S_a(T_1)$, PGV/PGD)	Vector			
13	($S_a(T_1)$, $S_a(T_1)^2$/AI)	Vector			

$S_d(T,5\%)$, $S_v(T,5\%)$, and $S_a(T,5\%)$ are the 5% damped displacement, pseudo-velocity, and pseudo-acceleration response spectra, respectively. $a(t)$ is the amplitude of the acceleration at time t and $t_{\max}$ is the total duration of the ground motion record.

Table 2 Design ID numbers and fundamental periods of the structures

Number of stories	Design ID	Fundamental period (s)
2	2064	0.66
4	1003	1.12
8	1011	1.71
12	1013	2.01
20	1021	2.36

(IDA) (Vamvatsikos and Cornell, 2002). The IDA curves of the structural response show the engineering demand parameter (EDP), considered to be the maximum interstory drift ratio, versus the IM_1 level. To perform IDA, IM_1 should be increased until the IM_1 capacity (IM_{1Cap}) associated with the target EDP level is reached for each ground motion record. Then, it is possible to determine the effects of IM_2 on the distribution of IM_{1Cap} values. IM_2 can explain part of the variation of IM_{1Cap}, thus, the probability of exceeding the IM_{1Cap} associated with the target EDP level can be expressed in terms of a conditional distribution of IM_{1Cap} given IM_2 (Baker, 2005). Assuming the conditional distribution of $\ln IM_{1Cap}$ to be linearly dependent on $\ln IM_2$ (ln represents the natural logarithm), Eq. (3) can be used to find the conditional mean of $\ln IM_{1Cap}$ given IM_2.

$$\mu_{\ln IM_{1Cap}|IM_2=im_2} = \alpha_0 + \alpha_1 \ln IM_2 \tag{3}$$

where α_0 and α_1 are coefficients to be estimated from linear regression. Note that when ε_{Sa} is used as IM_2, the term $\ln IM_2$ in Eq. (3) should be replaced with IM_2. The conditional standard deviation of $\ln IM_{1Cap}$ given IM_2 ($\sigma_{\ln IM_{1Cap}|IM_2}$) can be estimated by computing the standard deviation of the regression residuals as follows:

$$\sigma_{\ln IM_{1Cap}|IM_2} = \left[\sum_{i=1}^{n} (\ln IM_{1Cap_i} - \ln \overline{IM}_{1Cap_i})^2 / (n-2) \right]^{\frac{1}{2}} \tag{4}$$

where $\ln IM_{1Cap_i}$ is the natural logarithm of the IM_{1Cap} value obtained for the ground motion record i, and $\ln \overline{IM}_{1Cap_i}$ is the conditional mean of $\ln IM_{1Cap}$ given IM_2 that can be obtained by Eq. (3) for each ground motion record.

In this study, the collapse of structures was considered as the target EDP level, and $S_a(T_1)$ was used as IM_1 for the scaling of records. Therefore, the collapse capacity ($S_{a_{col}}$) is identical to the IM_{1Cap} associated with collapse. To obtain the collapse capacities of the structures, IDAs were performed by using the selected ground motion set. The amplitude of each record in the set, $S_a(T_1)$, was scaled to an increasing intensity until it causes collapse. Collapse was assumed to take place when dynamic instability occurs and the IDA curve becomes flat (Villaverde, 2007). Thus, the collapse capacity corresponding to each ground motion record ($S_{a_{col}}$) was obtained. In the IDA approach, the hunt and fill algorithm (Vamvatsikos and Cornell, 2002) was used to obtain the collapse capacities corresponding to all of the ground motion records. Figure 1 presents the results of the IDAs for the 12-story structure.

To validate the linear relation assumed in Eq. (3), the p-values from the F-test (Ang and Tang, 1975) for the regression coefficient (α_1) were calculated considering all of the IM_2 parameters presented in Table 1. The results indicated that all of the p-values were less than 0.05, which implies the statistical significance of α_1 and confirms the validity of this assumption (e.g., see the p-values for different IM_2 parameters presented in Fig. 2).

According to Baker (2005), the method described in this section, which is recognized as the capacity method, and other methods (e.g., stripe and cloud methods) can be used for seismic collapse assessment of structures; he found that the stripe and capacity methods produced approximately equivalent results. As pointed out by Baker (2005) and Rajeev *et al.* (2008), the capacity method requires reduced computational effort compared with the stripe method and avoids the need to treat separately the records that cause collapse.

4 Efficiency of the IMs for collapse capacity prediction

When using a scalar IM to estimate the IM capacity values by the IDA approach, the observed capacity dispersion is closely connected to the IM used (e.g., PGA or $S_a(T_1)$). A scalar IM is more efficient for IM capacity (e.g., collapse capacity) prediction if it indicates lower dispersion of the IM capacity values (Vamvatsikos and Cornell, 2005; Tothong and Luco, 2007; Iervolino and Manfredi, 2008). Therefore, it can be inferred that when using a vector-valued IM for collapse capacity prediction, the efficiency of the vector-valued IM is gauged by the degree of scatter about the regression in Eq. (3). The scatter about the regression

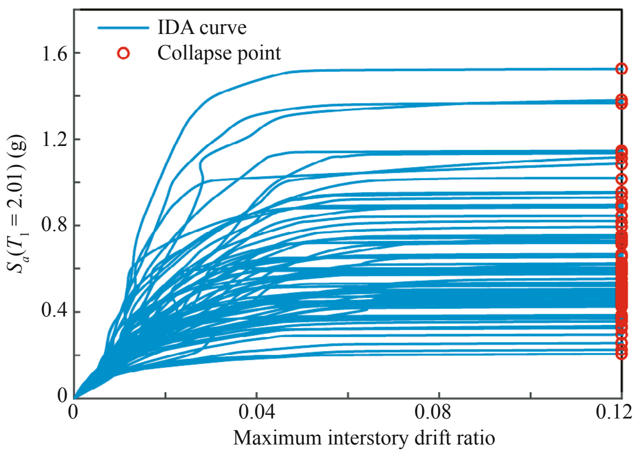

Fig. 1 IDA curves obtained for the 12-story structure

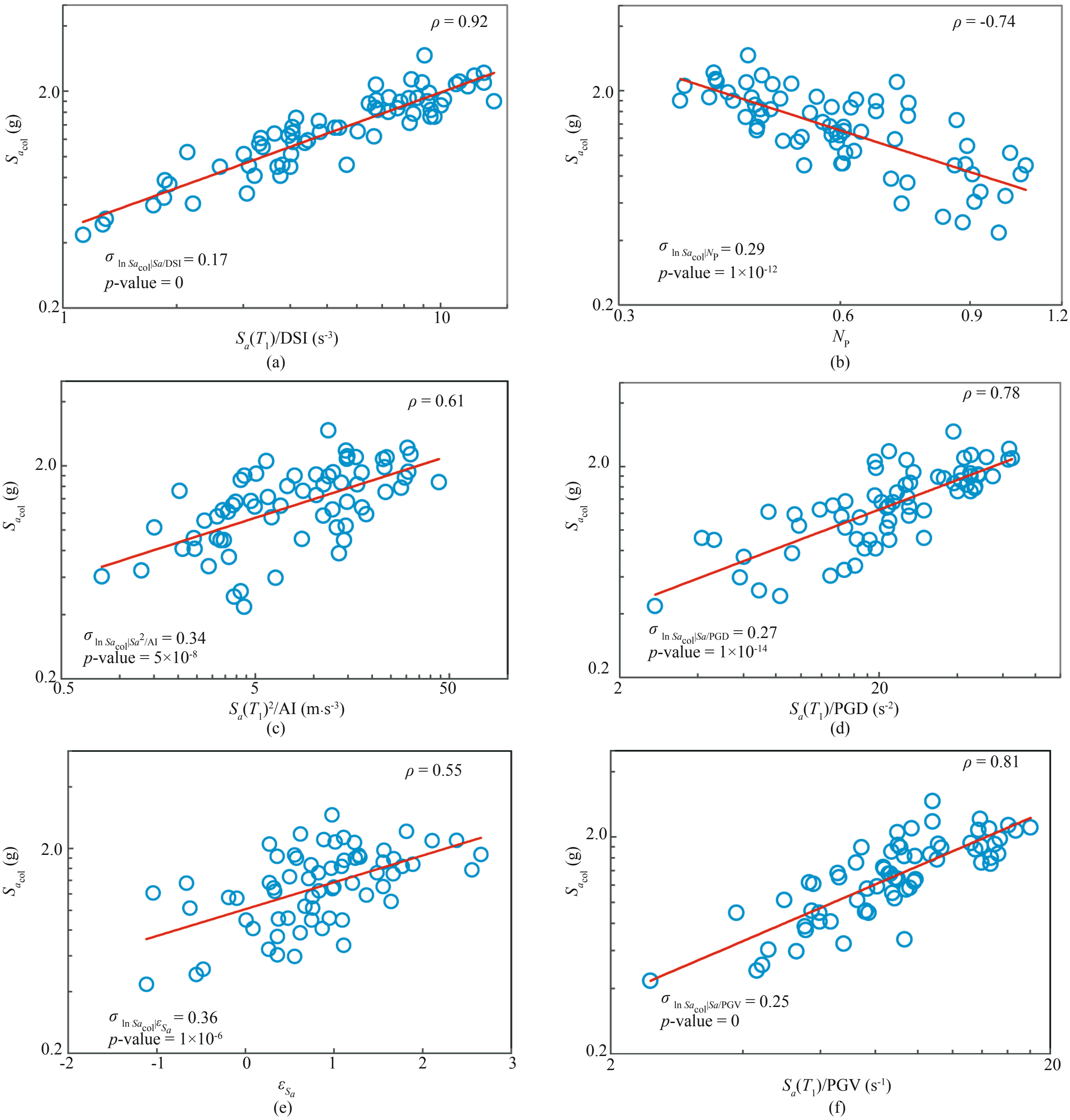

Fig. 2 Correlation between the collapse capacity of the 4-story structure and different IM_2 parameters: (a) $S_a(T_1)$/DSI, (b) N_p, (c) $S_a(T_1)^2$/AI, (d) $S_a(T_1)$/PGD, (e) ε_{S_a}, and (f) $S_a(T_1)$/PGV

fit can be quantified by using Eq. (4). In other words, a vector-valued IM, which includes $S_a(T_1)$ as IM_1, is more efficient for collapse capacity prediction, if it causes a lower conditional standard deviation of $\ln S_{a_{col}}$ ($\sigma_{\ln Sa_{col}|IM_2}$). Having a low scatter about the regression (of $\ln S_{a_{col}}$ on $\ln IM_2$) fit means that $\ln S_{a_{col}}$ and $\ln IM_2$ are highly correlated. Therefore, the size of correlation can be an index of the efficiency of a vector-valued IM for collapse capacity prediction. The correlation coefficient between two random variables, the natural logarithm of the structural collapse capacity ($\ln S_{a_{col}}$) and $\ln IM_2$ can be calculated as follows:

$$\rho = \frac{\mathrm{cov}(\ln S_{a_{col}}, \ln IM_2)}{\sigma_{\ln Sa_{col}}\sigma_{\ln IM_2}} \tag{5}$$

where cov() represents the covariance between two random variables; $\sigma_{\ln Sa_{col}}$ and $\sigma_{\ln IM_2}$ and are the standard deviations of $\ln S_{a_{col}}$ and $\ln IM_2$, respectively.

Figure 2 shows the correlation between $\ln S_{a_{col}}$ and $\ln IM_2$ considering different IM_2 parameters for the

4-story structure. As shown in this figure, using the ratio of two scalar IMs as the second component of a vector-valued IM can result in more efficient vector-valued IMs for predicting the structural collapse capacity, such as ($S_a(T_1)$, $S_a(T_1)$/DSI), ($S_a(T_1)$, $S_a(T_1)$/PGV), and ($S_a(T_1)$, $S_a(T_1)$/PGD), in comparison with the well-known vector-valued IMs (i.e., ($S_a(T_1)$, N_p) and ($S_a(T_1)$, ε_{Sa})). Gehl *et al.* (2013) also mentioned that, to obtain an efficient IM, the ratio of two scalar IMs can be used as a component in a vector-valued IM.

Table 3 presents the correlation coefficients between the values of ln $S_{a\mathrm{col}}$ obtained for the structures and the corresponding ln IM$_2$ values of the vector-valued IMs. It should be noted that when ε_{Sa} was used as IM$_2$, the correlation coefficient was obtained between the values of ln $S_{a\mathrm{col}}$ and the corresponding ε_{Sa} values. As shown in this table, $S_a(T_1)$/DSI as IM$_2$ has higher correlation with the collapse capacity of the structures when compared with the other IM$_2$ parameters. According to the results, in addition to the vector ($S_a(T_1)$, $S_a(T_1)$/DSI) that is the most efficient IM, using the vector ($S_a(T_1)$, $S_a(T_1)$/PGD) can also cause acceptable efficiency for collapse capacity prediction of the structures. It should be noted that the efficiency of ($S_a(T_1)$, N_p) for collapse capacity prediction increases with increasing structural height. The results also indicate that using the vector ($S_a(T_1)$, $S_a(T_1)^2$/AI), which accounts for the energy content of ground motion records, does not result in considerable efficiency for collapse capacity prediction of the structures.

To compare the efficiency of the vector-valued IMs graphically, the values of $\sigma_{\ln Sa_{\mathrm{col}}|\mathrm{IM}_2}$ obtained for the structures, considering different vector-valued IMs, are presented in Figure 3. The values of $\sigma_{\ln Sa_{\mathrm{col}}}$ are also presented in this figure to ease a good comparison. It can be seen that the minimum value of $\sigma_{\ln Sa_{\mathrm{col}}|\mathrm{IM}_2}$ was achieved by using the vector ($S_a(T_1)$, $S_a(T_1)$/DSI) for all of the structures. Consequently, the higher correlation coefficient for $S_a(T_1)$/DSI represents a lower $\sigma_{\ln Sa_{\mathrm{col}}|\mathrm{IM}_2}$ and hence a more efficient vector-valued IM for collapse capacity prediction.

The use of an efficient vector-valued IM in seismic performance assessment of structures increases the reliability of the assessment. In other words, using an efficient IM can considerably reduce the number of analyses required for the estimation of structural response or capacity with a given accuracy. By applying a vector-valued IM that includes $S_a(T_1)$ as the first component, the conditional standard deviation of ln $S_{a\mathrm{col}}$ ($\sigma_{\ln Sa_{\mathrm{col}}|\mathrm{IM}_2}$) can be obtained. Then, the standard error of the collapse capacity associated with a sample of size n_s can be expressed as:

$$\mathrm{SE} = \frac{\sigma_{\ln Sa_{\mathrm{col}}|\mathrm{IM}_2}}{\sqrt{n_s}} \tag{6}$$

According to Eq. (6), by applying a more efficient IM, the sample size, n_s, can be reduced while the standard error remains the same, which means that lower effort and computational expense are needed for collapse assessment. When using $S_a(T_1)$ as a scalar IM,

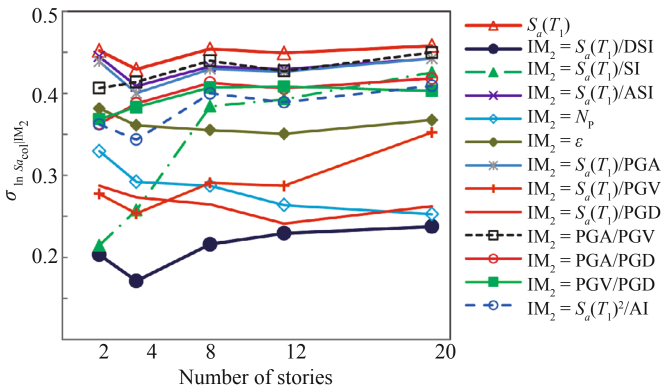

Fig. 3 Values of $\sigma_{\ln Sa_{\mathrm{col}}|\mathrm{IM}_2}$ obtained for the structures considering different vector-valued IMs

Table 3 Correlation coefficients between the values of ln Sa_{col} obtained for the structures and the corresponding ln IM$_2$ values

IM$_2$	2-Story	4-Story	8-Story	12-Story	20-Story
$S_a(T_1)$/DSI	0.895	0.918	0.882	0.862	0.857
$S_a(T_1)$/SI	0.882	0.803	0.543	0.497	0.387
$S_a(T_1)$/ASI	0.215	0.326	0.325	0.316	0.284
N_p	-0.691	-0.737	-0.778	-0.812	-0.837
ε_{Sa}	0.547	0.551	0.630	0.632	0.606
$S_a(T_1)$/PGA	0.271	0.379	0.344	0.334	0.285
$S_a(T_1)$/PGV	0.793	0.810	0.772	0.772	0.646
$S_a(T_1)$/PGD	0.776	0.775	0.816	0.846	0.823
PGA/PGV	0.452	0.291	0.278	0.330	0.225
PGA/PGD	0.605	0.443	0.431	0.442	0.423
PGV/PGD	0.588	0.464	0.457	0.430	0.488
$S_a(T_1)^2$/AI	0.607	0.607	0.487	0.510	0.463

the term $\sigma_{\ln Sa_{\mathrm{col}}|\mathrm{IM}_2}$ in Eq. (6) should be replaced with the standard deviation of ln $S_{a_{\mathrm{col}}}$ ($\sigma_{\ln Sa_{\mathrm{col}}}$).

As an example of the effect of IM efficiency on increasing the reliability of the analyses, in the case of the 8-story structure, the use of $S_a(T_1)$ as a scalar IM led to a $\sigma_{\ln Sa_{\mathrm{col}}}$ value of 0.454, whereas using the vectors ($S_a(T_1)$, N_{P}) and ($S_a(T_1)$, $S_a(T_1)$/DSI) led to $\sigma_{\ln Sa_{\mathrm{col}}|\mathrm{IM}_2}$ values of 0.287 and 0.216, respectively. Thus, according to Eq. (6), considering the same standard error, the number of required analyses can be decreased about 4.4 times with the use of the vector ($S_a(T_1)$, $S_a(T_1)$/DSI) instead of $S_a(T_1)$. Also, by using the vector ($S_a(T_1)$, N_{P}) instead of $S_a(T_1)$, the number of required analyses can be decreased about 2.5 times. According to Haselton *et al*. (2011) and Haselton and Deierlein (2008), the obtained logarithmic standard deviation of the collapse capacity ($\sigma_{\ln Sa_{\mathrm{col}}}$) for the 8-story structure was equal to 0.45, which confirms the value obtained in this study.

In other performance levels, such as life safety, in which the response of the structure becomes moderately nonlinear, the efficiency of IMs may vary. To investigate this issue, the $\mathrm{IM}_{\mathrm{1Cap}}$ values associated with the life safety target EDP level ($S_{a_{\mathrm{ls}}}$) were obtained for all of the structures. The life safety target EDP level was defined as a maximum interstory drift ratio of 2% for reinforced concrete moment resisting frames (ASCE 41-06, 2007). Table 4 presents the results of the analyses carried out for the life safety performance level. As indicated in this table, N_{P} , which has moderate efficiency for collapse capacity prediction in comparison with the other IM_2 parameters, is more efficient than $S_a(T_1)$/DSI for predicting $S_{a_{\mathrm{ls}}}$ in most of the structures. Therefore, it can be inferred that in performance levels related to moderate levels of nonlinearity, such as life safety, the vector ($S_a(T_1)$, N_{P}) may be more efficient than ($S_a(T_1)$, $S_a(T_1)$/DSI) for predicting the $\mathrm{IM}_{\mathrm{1Cap}}$ values. Actually, the efficiency of an IM is dependent on the severity of the nonlinear response, and one IM that is the most efficient in different performance levels cannot be found. Although the vector ($S_a(T_1)$, $S_a(T_1)$/DSI) is not the most efficient IM in the life safety performance level, it is the most efficient one for collapse capacity prediction and has acceptable efficiency in the life safety performance level.

5 Sufficiency of the IMs for collapse capacity prediction

5.1 Sufficiency with respect to magnitude and source-to-site distance

A sufficient IM produces the same distribution of demands and capacities independently of the ground motion selection (Vamvatsikos and Cornell, 2005; Tothong and Luco, 2007). The sufficiency of a scalar IM for collapse capacity prediction means that the distribution of collapse capacity obtained by using the IM is independent of ground motion characteristics, such as earthquake magnitude (M) and source-to-site distance (R). Because the distribution of collapse capacity is obtained from the results of a finite number of IDAs, sufficiency is one of the important properties of an optimal IM. Thus, if this distribution is dependent on the M and R values of the ground motions used, then the distribution will be biased if the distribution of the M and R of the ground motions used in the IDAs is not the same as that of the ground motions that will occur at the site in the future (Bradley *et al*., 2010). As pointed out by Bojórquez and Iervolino (2011), sufficiency of an IM is important because a sufficient IM can be used in probabilistic structural assessment decoupling the hazard and structural analysis.

To examine the sufficiency of $S_a(T_1)$ as a scalar IM with respect to M and R for predicting the collapse capacity of structures, linear regression can be performed between these properties of ground motions and the observed collapse capacities from the IDAs by using the

Table 4 Correlation coefficients between the values of ln $S_{a_{\mathrm{ls}}}$ obtained for the structures and the corresponding ln IM_2 values

IM_2	2-Story	4-Story	8-Story	12-Story	20-Story
$S_a(T_1)$/DSI	0.583	0.625	0.793	0.788	0.810
$S_a(T_1)$/SI	0.800	0.833	0.557	0.512	0.335
$S_a(T_1)$/ASI	0.216	0.386	0.312	0.287	0.241
N_{P}	-0.792	-0.757	-0.771	-0.799	-0.812
ε_{Sa}	0.339	0.374	0.543	0.569	0.520
$S_a(T_1)$/PGA	0.309	0.452	0.361	0.319	0.266
$S_a(T_1)$/PGV	0.711	0.746	0.755	0.773	0.657
$S_a(T_1)$/*PGD*	0.564	0.572	0.701	0.730	0.780
PGA/PGV	0.334	0.133	0.236	0.353	0.266
PGA/PGD	0.376	0.208	0.320	0.357	0.404
PGV/PGD	0.320	0.222	0.314	0.275	0.424
$S_a(T_1)^2$/AI	0.4071	0.5241	0.4240	0.4562	0.3706

following equation:

$$\mu_{\ln Sa_{col}} = \beta_0 + \beta_1 x \quad (7)$$

where $\mu_{\ln Sa_{col}}$ is the expected value of $\ln S_{a_{col}}$; β_0 and β_1 are coefficients to be estimated from linear regression; and x is one of the parameters M or the natural logarithm of R (ln$R$). Because the linear regression is based on a finite number of observations, it is essential to use statistical tests to determine the significance of the coefficient β_1. Assuming a Student-*t* distribution for the coefficient β_1, the F-test can be used to determine the statistical significance of β_1 (Ang and Tang, 1975). In general, a p-value less than 0.05 obtained from the F-test indicates that the slope of the linear regression (β_1) is a statistically significant value, which represents the insufficiency of $S_a(T_1)$ with respect to x. To examine the sufficiency of the vector-valued IMs for collapse capacity prediction, the residuals of the collapse capacities, obtained considering the linear regression on the second component of each vector-valued IM (Eq. (3)), were used in Eq. (7) instead of the collapse capacities. Other researchers (e.g., Luco and Cornell, 2007; Baker and Cornell, 2008a; Tothong and Cornell, 2008; Bradley *et al.*, 2009a) also applied structural response residuals to test the sufficiency of different IMs.

Figure 4 shows the results of testing the sufficiency of $S_a(T_1)$ as a scalar IM with respect to M and R for collapse capacity prediction of the 4-story structure. As shown in this figure, $S_a(T_1)$ is insufficient with respect to M because the p-value obtained from the F-test is less than 0.05, whereas it is sufficient with respect to R because the corresponding p-value is greater than 0.05. In other words, $S_a(T_1)$ is unable to fully account for the effect of magnitude and thus for reliable seismic collapse assessment of this structure by using $S_a(T_1)$ as a scalar IM, the magnitude of ground motions should be considered in the ground motion selection process. However, the source-to-site distance of ground motions does not need to be considered as a determining factor in ground motion selection. As an alternative, the use of a sufficient IM with respect to M can eliminate the need to consider magnitude as an important criterion in the ground motion selection for seismic analyses. Table 5 presents the results of investigating the sufficiency of $S_a(T_1)$ with respect to M and R for collapse capacity prediction of the structures. As shown in this table, $S_a(T_1)$ is insufficient with respect to M, whereas it is sufficient with respect to R. The effect of magnitude may be accounted for by adding a proper parameter to $S_a(T_1)$ and developing a vector-valued IM.

Figure 5 compares the sufficiency of the vectors ($S_a(T_1)$, $S_a(T_1)$/DSI) and ($S_a(T_1)$, N_p) with respect to M for collapse capacity prediction of the 4-story structure. It can be seen that for predicting the collapse capacity of the 4-story structure, ($S_a(T_1)$, $S_a(T_1)$/DSI) is sufficient with respect to M, whereas ($S_a(T_1)$, N_p) is insufficient. Table 6 presents the results of investigating the sufficiency of the vector-valued IMs with respect to M for collapse capacity prediction of the structures. The results show that $S_a(T_1)$/DSI as the second component of the vector ($S_a(T_1)$, $S_a(T_1)$/DSI) is able to account for the effect of magnitude for collapse capacity prediction of the structures. The other IM$_2$ parameters, except PGA/PGD and PGV/PGD, are unable to account for the effect of magnitude for predicting the collapse capacity of

Table 5 *P*-values obtained from investigating the sufficiency of $S_a(T_1)$ with respect to magnitude, source-to-site distance, and scale factor for collapse capacity prediction of the structures (*p*-values > 0.05 are marked in bold)

Structure	Sufficiency with respect to		
	M	*R*	Scale factor
2-Story	0.045	**0.607**	0.001
4-Story	0.008	**0.756**	0.002
8-Story	0.003	**0.787**	0.001
12-Story	0.009	**0.774**	0.032
20-Story	0.005	**0.635**	0.013

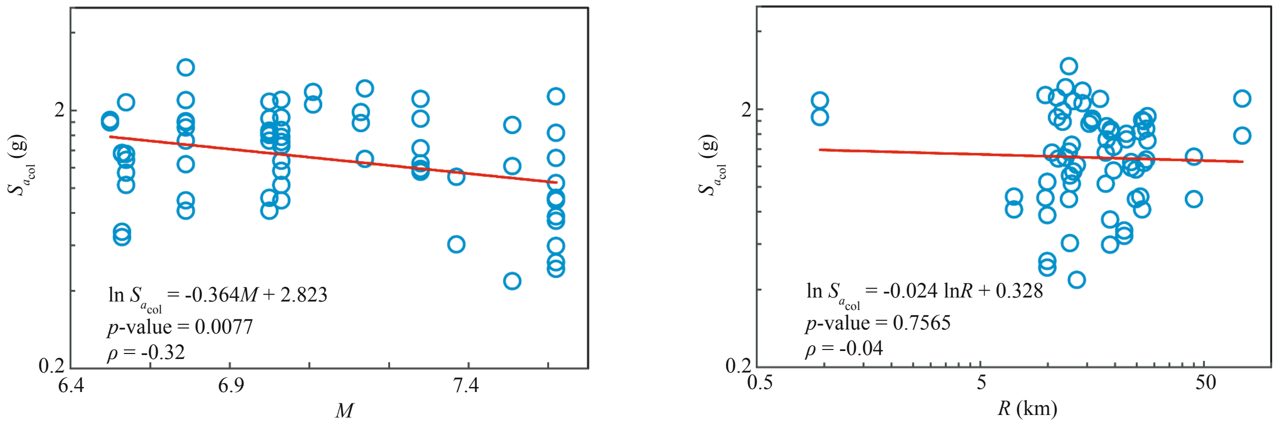

Fig. 4 Testing the sufficiency of $S_a(T_1)$ with respect to *M* and *R* for collapse capacity prediction of the 4-story structure: (a) *M* and (b) *R*

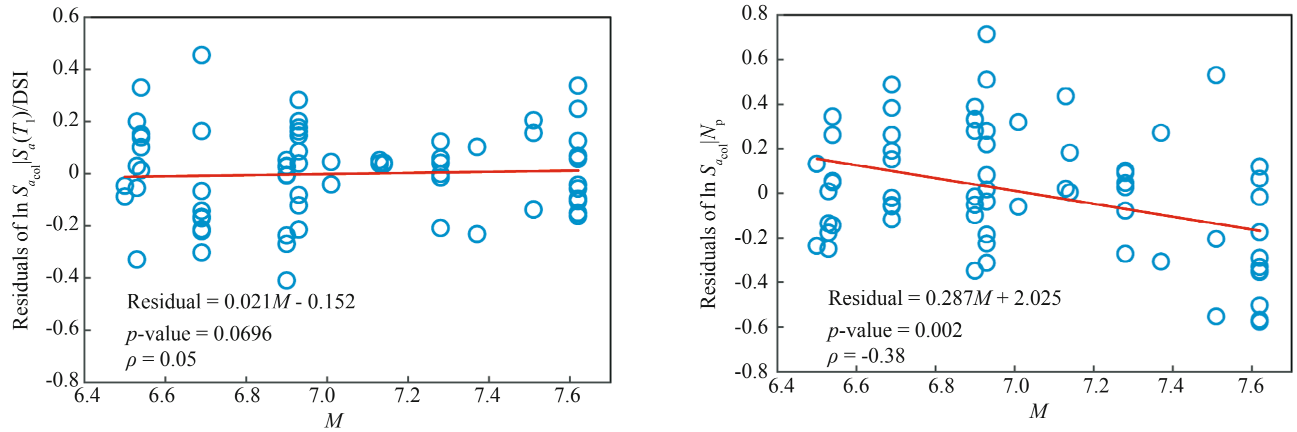

Fig. 5 **Testing the sufficiency of vector-valued IMs with respect to *M* for collapse capacity prediction of the 4-story structure: (a) ($S_a(T_1)$, $S_a(T_1)$/DSI) and (b) ($S_a(T_1)$, N_p)**

Table 6 ***P*-values obtained from investigating the sufficiency of the vector-valued IMs with respect to magnitude for collapse capacity prediction of the structures (*p*-values > 0.05 are marked in bold)**

Vector-valued IM	2-Story	4-Story	8-Story	12-Story	20-Story
($S_a(T_1)$, $S_a(T_1)$/DSI)	**0.108**	**0.696**	**0.859**	**0.981**	**0.864**
($S_a(T_1)$, $S_a(T_1)$/SI)	0.008	0.000	0.000	0.000	0.000
($S_a(T_1)$, $S_a(T_1)$/ASI)	0.023	0.001	0.000	0.001	0.000
($S_a(T_1)$, N_p)	**0.065**	0.002	**0.079**	**0.176**	**0.698**
($S_a(T_1)$, ε_{Sa})	0.015	0.006	0.004	0.007	0.005
($S_a(T_1)$, $S_a(T_1)$/PGA)	0.030	0.002	0.000	0.001	0.001
($S_a(T_1)$, $S_a(T_1)$/PGV)	**0.703**	**0.207**	0.014	0.002	0.002
($S_a(T_1)$, $S_a(T_1)$/PGD)	0.046	**0.270**	**0.321**	**0.224**	**0.506**
($S_a(T_1)$, PGA/PGV)	**0.458**	**0.064**	0.025	**0.092**	0.029
($S_a(T_1)$, PGA/PGD)	**0.476**	**0.412**	**0.220**	**0.452**	**0.284**
($S_a(T_1)$, PGV/PGD)	**0.501**	**0.492**	**0.281**	**0.445**	**0.453**
($S_a(T_1)$, $S_a(T_1)^2$/AI)	0.015	0.000	0.000	0.000	0.000

some or all of the structures. As an example, the vector ($S_a(T_1)$, $S_a(T_1)$/PGD), which has acceptable efficiency, is not sufficient with respect to *M* when applied for the 2-story structure. It should be noted that the vectors ($S_a(T_1)$, PGA/PGD) and ($S_a(T_1)$, PGV/PGD), which are sufficient with respect to *M*, do not have considerable efficiency for collapse capacity prediction. The results also indicate that the degree of sufficiency of some of the vector-valued IMs with respect to *M* varies with the dynamic characteristics of the structures. For example, the vector ($S_a(T_1)$, N_p) has lower sufficiency for the low- to mid-rise structures in comparison with the taller structures.

Another parameter with respect to which an optimal IM should be sufficient is the source-to-site distance (*R*) of the ground motion. As shown in Fig. 4 and Table 5, $S_a(T_1)$ is sufficient with respect to *R* for collapse capacity prediction of the structures. Hence, investigating the sufficiency with respect to *R* is not necessary for vector-valued IMs in which the first component is $S_a(T_1)$.

5.2 Sufficiency with respect to scale factor

One of the desirable features of an optimal IM is scaling robustness, which represents sufficiency with respect to scale factor. A number of researchers (e.g., Baker, 2005; Bradley *et al.*, 2010) have recently studied the scaling robustness of different IMs. As described previously, to obtain the collapse capacities through the IDA approach, the records should be scaled to increasing $S_a(T_1)$ levels until the collapse occurs. Therefore, the sufficiency of the considered IMs with respect to scale factor for collapse capacity prediction is an important issue because it removes the potential bias due to scaling in the prediction of structural collapse capacity. To investigate the sufficiency of the IMs with respect to scale factor for collapse capacity prediction, the method described in Section 5.1 was applied by replacing the parameter *x* in Eq. (7) with the natural logarithm of scale factor (lnSF). Figure 6 shows that $S_a(T_1)$ is not sufficient with respect to scale factor for predicting

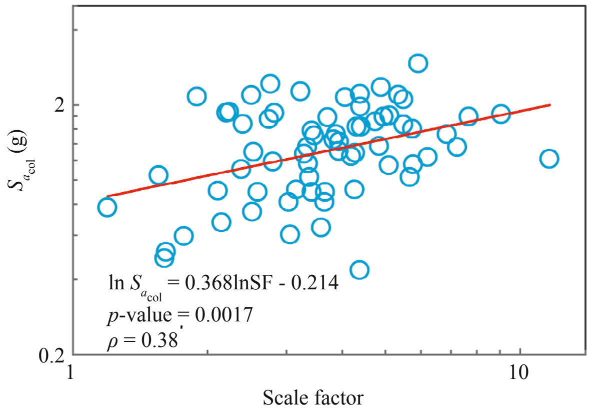

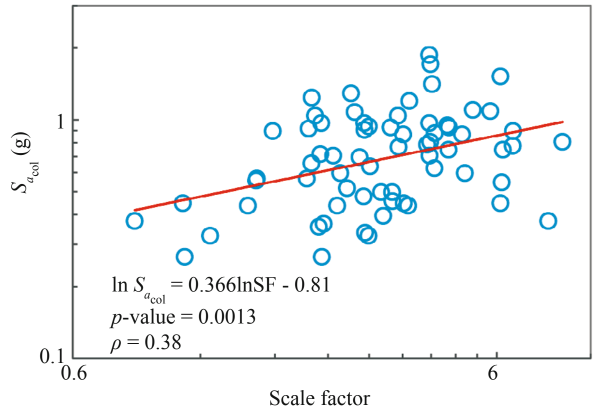

Fig. 6 Testing the sufficiency of $S_a(T_1)$ with respect to scale factor for collapse capacity prediction of: (a) the 4-story structure and (b) the 8-story structure

the collapse capacities of the 4- and 8-story structures, having p-values of less than 0.05.

Table 5 presents the results of investigating the sufficiency of $S_a(T_1)$ with respect to scale factor for collapse capacity prediction of the structures. The findings show that $S_a(T_1)$ as a scalar IM is not sufficient with respect to scale factor. Table 7 presents the results of investigating the sufficiency of the vector-valued IMs with respect to scale factor for collapse capacity prediction of the structures. As shown in this table, the vector ($S_a(T_1)$, $S_a(T_1)$/DSI) is sufficient with respect to scale factor for collapse capacity prediction of the structures; the vector ($S_a(T_1)$, N_p) is not sufficient with respect to scale factor for predicting the collapse capacity of the 2-story structure, but it is sufficient for the taller structures. Furthermore, the vector ($S_a(T_1)$, $S_a(T_1)$/PGD), which is not sufficient with respect to scale factor for collapse capacity prediction of the low-rise structures, is sufficient for the mid- to high-rise structures.

6 Predicting the probability of collapse through logistic regression

Logistic regression (Kutner *et al.*, 2005) is a commonly used tool for analyzing binary data (e.g., collapse/non-collapse). Given a specific value for the first component of a vector-valued IM (IM_1), logistic regression can be used to predict the probability of collapse as a function of IM_2. In this procedure, the records are scaled to a specific level of IM_1, and the response of the structure (e.g., maximum interstory drift ratio) is divided into two groups of collapse and non-collapse responses. Then, noting that each record has a value of IM_2, which can be used as the predictor variable, the probability of collapse (P_C) can be calculated through logistic regression. Using the indicator variable C to designate the occurrence of collapse (C equals 1 if the record causes collapse and 0 otherwise), the following functional form is fitted (Baker, 2005; Baker and Cornell,

Table 7 *P*-values obtained from investigating the sufficiency of the vector-valued IMs with respect to scale factor for collapse capacity prediction of the structures (*p*-values > 0.05 are marked in bold)

Vector-valued IM	2-Story	4-Story	8-Story	12-Story	20-Story
($S_a(T_1)$, $S_a(T_1)$/DSI)	**0.146**	**0.995**	**0.302**	**0.174**	**0.196**
($S_a(T_1)$, $S_a(T_1)$/SI)	0.003	0.000	0.000	0.000	0.000
($S_a(T_1)$, $S_a(T_1)$/ASI)	0.000	0.000	0.000	0.000	0.000
($S_a(T_1)$, N_p)	0.006	**0.205**	**0.862**	**0.500**	**0.383**
($S_a(T_1)$, ε_{Sa})	0.000	0.000	0.000	0.000	0.000
($S_a(T_1)$, $S_a(T_1)$/PGA)	0.000	0.000	0.000	0.000	0.000
($S_a(T_1)$, $S_a(T_1)$/PGV)	0.000	0.000	0.000	0.000	0.000
($S_a(T_1)$, $S_a(T_1)$/PGD)	0.001	0.009	**0.054**	**0.362**	**0.120**
($S_a(T_1)$, PGA/PGV)	**0.102**	**0.063**	**0.082**	**0.724**	**0.199**
($S_a(T_1)$, PGA/PGD)	**0.116**	**0.133**	**0.300**	**0.781**	**0.960**
($S_a(T_1)$, PGV/PGD)	0.008	0.030	**0.108**	**0.671**	**0.829**
($S_a(T_1)$, $S_a(T_1)^2$/AI)	0.000	0.000	0.000	0.000	0.000

2008b):

$$P_C = P(C|\mathrm{IM}_1 = \mathrm{im}_1, \mathrm{IM}_2 = \mathrm{im}_2) = \frac{e^{a+b\,\mathrm{im}_2}}{1+e^{a+b\,\mathrm{im}_2}} \tag{8}$$

where a and b are coefficients to be estimated from the logistic regression on a data set that contains C values indicating the collapse and non-collapse cases, and the corresponding IM_2 values. Due to the scaling of records to have a specific value of $\mathrm{IM}_1 = \mathrm{im}_1$, the coefficients a and b are implicitly dependent on IM_1. Thus, the fragility curve obtained from the logistic regression is a function of the first and second components of the considered vector-valued IM. For a given level of IM_1, the efficiency of IM_2 for seismic collapse assessment can be investigated by the shape of the fragility curve obtained from the logistic regression. A flat fragility curve indicates that IM_2 does not add any significant information to the collapse assessment, whereas a steep fragility curve indicates that IM_2 is efficient for seismic collapse assessment (Bojórquez *et al*., 2012). Figure 7 presents the collapse fragility curves obtained for the 4-story structure through logistic regression, at $S_a(T_1) = 1.2$ g, considering different vector-valued IMs. As illustrated in this figure, the steep shape of the fragility curve obtained using $S_a(T_1)$/DSI as the second component of the vector ($S_a(T_1)$, $S_a(T_1)$/DSI), indicates that $S_a(T_1)$/DSI is more efficient than the other IM_2 parameters for seismic collapse assessment of the structure.

7 Collapse fragility surfaces

The use of collapse fragility curves to assess the collapse safety of structures has recently become a common practice (e.g., Zareian, 2006; Haselton and Deierlein, 2008; Tang *et al*., 2011; Eads *et al*., 2013). The collapse fragility curve obtained by using a scalar IM shows how the probability of collapse of a structure increases with increasing IM level. In the case of vector-valued IMs, the collapse fragility surface can be obtained instead of the collapse fragility curve (Seyedi *et al*., 2010). In fact, one of the advantages of using vector-valued IMs is that the variation of the probability of collapse with respect to both components of a vector-valued IM can be obtained.

As pointed out by Baker (2005), if the conditional distribution of $\ln \mathrm{IM}_{1\mathrm{Cap}}$ given IM_2 is assumed to be Gaussian, then the conditional mean ($\mu_{\ln \mathrm{IM}_{1\mathrm{Cap}}|\mathrm{IM}_2=\mathrm{im}_2}$) and standard deviation ($\sigma_{\ln \mathrm{IM}_{1\mathrm{Cap}}|\mathrm{IM}_2}$) obtained from Eqs. (3) and (4) can define the conditional distribution of $\ln \mathrm{IM}_{1\mathrm{Cap}}$ for a given EDP level y. Therefore, the cumulative distribution function (CDF) of this conditional distribution can be calculated as:

$$P(\mathrm{IM}_{1\mathrm{Cap}} < \mathrm{im}_1 \,|\, \mathrm{EDP} = y, \mathrm{IM}_2 = \mathrm{im}_2) = \Phi\left(\frac{\ln \mathrm{im}_1 - \mu_{\ln \mathrm{IM}_{1\mathrm{Cap}}|\mathrm{IM}_2=\mathrm{im}_2}}{\sigma_{\ln \mathrm{IM}_{1\mathrm{Cap}}|\mathrm{IM}_2}}\right) \tag{9}$$

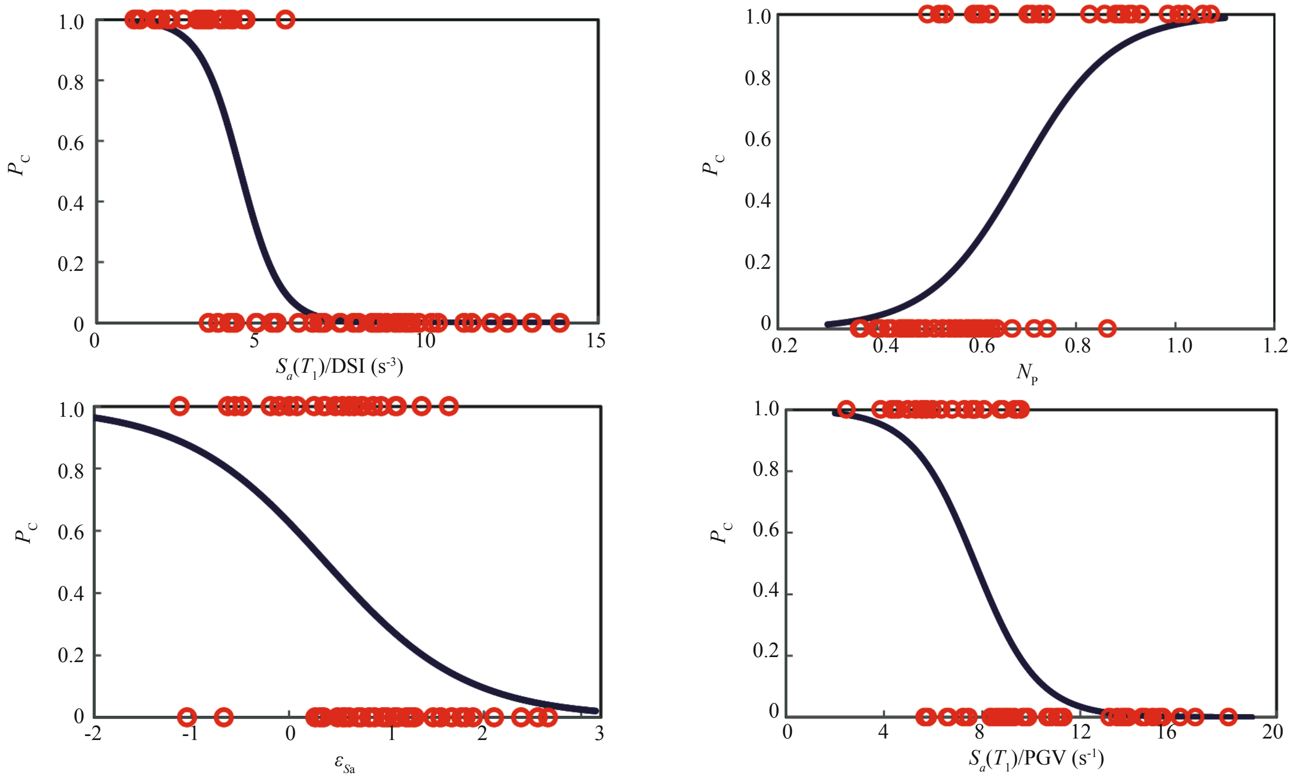

Fig. 7 Collapse fragility curves obtained for the 4-story structure through logistic regression at $S_a(T_1)$ = 1.2 g considering different vector-valued IMs

where $\Phi()$ is the CDF of the standard Gaussian distribution. Assuming EDP = y as the response level associated with collapse, and $S_a(T_1)$ as IM_1, Eq. (9) will be converted to Eq. (10). Thus, the collapse fragility surfaces considering different IM_2 parameters can be obtained as follows:

$$P(S_{a_{\mathrm{col}}} < S_a \mid \mathrm{collapse}, \mathrm{IM}_2 = \mathrm{im}_2) = \Phi\left(\frac{\ln S_a - \mu_{\ln Sa_{\mathrm{col}}|\mathrm{IM}_2=\mathrm{im}_2}}{\sigma_{\ln Sa_{\mathrm{col}}|\mathrm{IM}_2}}\right) \quad (10)$$

where $\mu_{\ln Sa_{\mathrm{col}}|\mathrm{IM}_2 = \mathrm{im}_2}$ and $\sigma_{\ln Sa_{\mathrm{col}}|\mathrm{IM}_2}$ are the conditional mean and standard deviation of $\ln S_{a_{\mathrm{col}}}$, respectively. Figure 8 presents the collapse fragility surfaces obtained for the 4-story structure considering different vector-valued IMs. As illustrated in this figure, the use of the vector ($S_a(T_1)$, $S_a(T_1)$/DSI), which is more efficient than the other IMs, leads to a steeper fragility surface in comparison with the use of the other IMs. Furthermore, the collapse fragility surface corresponding to a less efficient IM (e.g., ($S_a(T_1)$, ε_{Sa})) is flatter than those corresponding to more efficient IMs. Comparing the variation of the probability of collapse in the fragility surfaces with respect to IM_2 reveals that the largest variation exists in the fragility surface obtained by using ($S_a(T_1)$, $S_a(T_1)$/DSI) as a vector-valued IM. In other words, the probability of collapse is more sensitive to $S_a(T_1)$/DSI than to the other IM_2 parameters.

As mentioned by Gehl *et al*. (2013) and Seyedi *et al*. (2010), if two components of a vector-valued IM are highly correlated, then caution must be taken in the construction of the fragility surface and its interpretation. In fact, because of the high correlation between IM_1 and IM_2, the data points do not cover the whole 2D space defined by IM_1 and IM_2; thus, the definition of the fragility model for extreme values (e.g., low IM_1 and high IM_2) is questionable. In the case of uncorrelated components, performance assessment can be carried out in the whole 2D space defined by IM_1 and IM_2, even in the corners that contain high values of one parameter and low values of the second. Figure 9 shows the correlation between $S_a(T_1 = 1.12)$ ($T_1 = 1.12$ is the fundamental period of the 4-story structure) and the IM_2 parameters presented in Fig. 8, considering the ground motion set used in the structural analyses. It can be seen that $S_a(T_1)$ and $S_a(T_1)$/DSI have a relatively weak correlation (correlation coefficient of 0.45). Therefore, it can be assumed that the data points can cover the whole 2D space defined by $S_a(T_1)$ and $S_a(T_1)$/DSI.

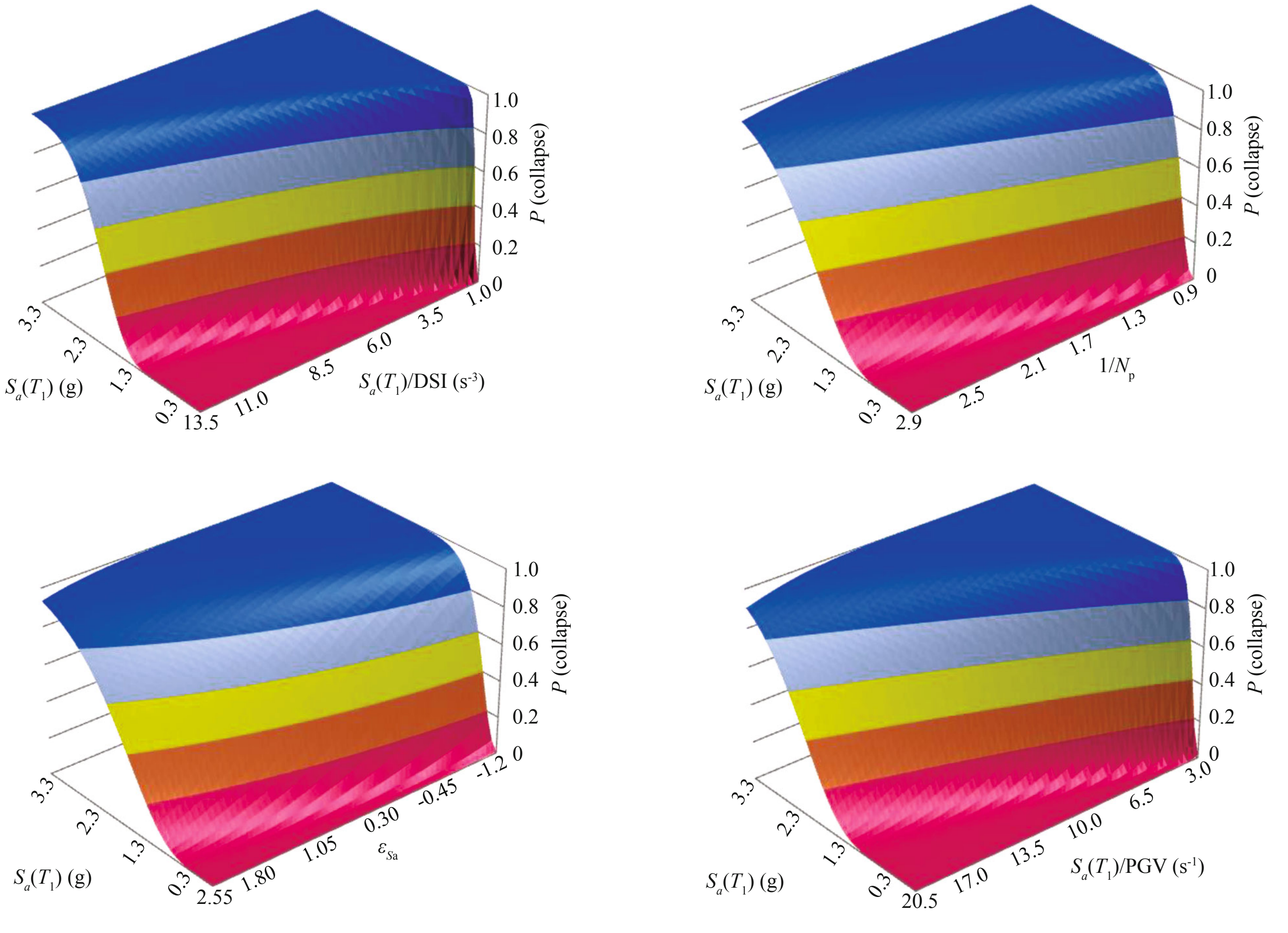

Fig. 8 Collapse fragility surfaces obtained for the 4-story structure considering different vector-valued IMs

According to the results presented in Sections 4 to 7, the vector ($S_a(T_1)$, $S_a(T_1)$/DSI) can be proposed as an optimal vector-valued IM for seismic collapse assessment of structures. Thus, to satisfy the predictability criterion for the proposed IM, a GMPE for its second component and the correlation between its components are provided in Section 8. It should be noted that further research can be carried out to investigate the performance of ($S_a(T_1)$, $S_a(T_1)$/DSI) for seismic collapse assessment of different types of structures (e.g., stiff low-rise or super-tall buildings).

8 Predictability of the proposed vector-valued IM

To perform VPSHA with the use of the proposed vector-valued IM, ($S_a(T_1)$, $S_a(T_1)$/DSI), both components of the IM should be predictable, and the correlation between $\ln S_a(T_1)$ and $\ln(S_a(T_1)/\mathrm{DSI})$ should be determined.

8.1 Ground motion prediction equation for $S_a(T)$/DSI

One of the features of an optimal IM is predictability; thus, to use ($S_a(T_1)$, $S_a(T_1)$/DSI) as an optimal vector-valued IM, the parameter $S_a(T)$/DSI should have a GMPE. Assuming $S_a(T)$/DSI to be lognormally distributed, it can be predicted based on the GMPEs currently available for $S_a(T)$ and DSI (the appropriateness of this assumption is verified in Section 8.2). Thus, the logarithmic mean and standard deviation of $S_a(T)$/DSI can be calculated as follows:

$$\mu_{\ln(Sa(T)/\mathrm{DSI})} = \mu_{\ln Sa(T)} - \mu_{\ln \mathrm{DSI}} \tag{11}$$

$$\sigma_{\ln(Sa(T)/\mathrm{DSI})} = \sqrt{(\sigma_{\ln Sa(T)})^2 + (\sigma_{\ln \mathrm{DSI}})^2 - 2\rho_{\ln Sa(T),\ln \mathrm{DSI}}\,\sigma_{\ln Sa(T)}\,\sigma_{\ln \mathrm{DSI}}} \tag{12}$$

where $\mu_{\ln Sa(T)}$ and $\sigma_{\ln Sa(T)}$ are the mean and standard deviation of $\ln S_a(T)$, respectively; $\mu_{\ln\ \mathrm{DSI}}$ and $\sigma_{\ln\ \mathrm{DSI}}$ are the mean and standard deviation of ln DSI, respectively; and $\rho_{\ln Sa(T),\ln \mathrm{DSI}}$ is the correlation between $\ln S_a(T)$ and ln DSI that can be obtained by using the relationship proposed by Bradley (2011a), as follows:

$$\rho_{\ln Sa(T),\ln \mathrm{DSI}} = \frac{a_n + b_n}{2} - \frac{a_n - b_n}{2}\tanh[d_n \ln(T/c_n)] \qquad e_{n-1} \le T < e_n \tag{13}$$

where $\tanh[]$ is the hyperbolic tangent function; a_n, b_n, c_n, and d_n are empirical constants used for piece-wise

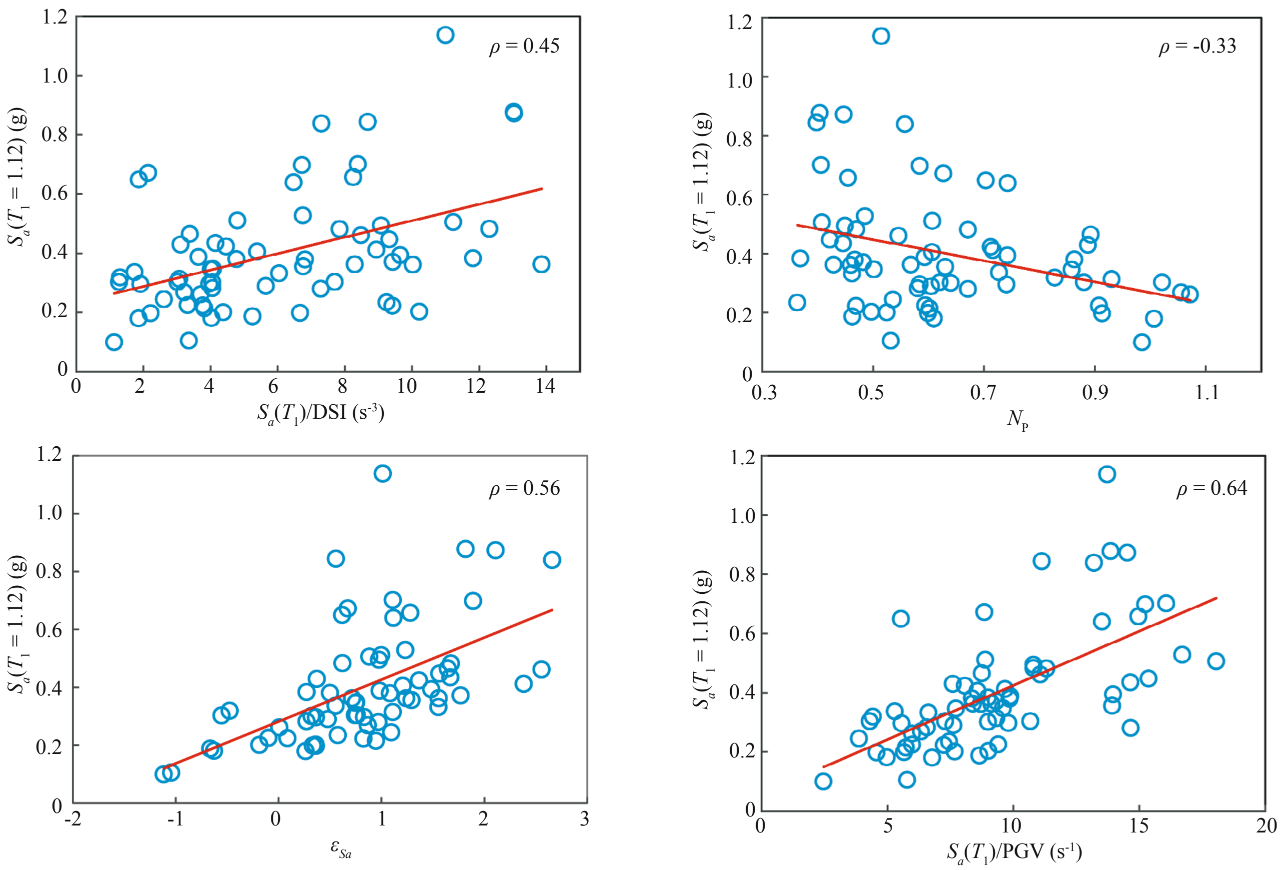

Fig. 9 Correlation between $S_a(T_1 = 1.12)$ and different IM$_2$ parameters considering the ground motion set used in the structural analyses: (a) $S_a(T_1)$/DSI , (b) N_p, (c) ε_{Sa}, and (d) $S_a(T_1)$/PGV

segment n; and e_n defines the period range for each of the piece-wise segments. Table 8 provides the numerical values of the parameters in Eq. (13) for obtaining the correlation between $\ln S_a(T)$ and $\ln$ DSI.

8.2 Obtaining the correlation between $\ln S_a(T)$ and $\ln (S_a(T)/\mathrm{DSI})$

According to the method proposed by Bazzurro and Cornell (2002), when using ($S_a(T_1)$, $S_a(T_1)$/DSI) in VPSHA, the correlation between $\ln S_a(T_1)$ and $\ln (S_a(T_1)/\mathrm{DSI})$ should be determined. In this study, a set containing 350 horizontal ground motion records (including the 67 records used for the analysis of the structures) related to shallow crustal earthquakes was selected for obtaining the correlation between $\ln S_a(T)$ and $\ln (S_a(T)/\mathrm{DSI})$ in different periods. Baker (2005) used a ground motion set to investigate the correlation of response spectral values. Some of the criteria considered in the selection of this ground motion set were as follows: the ground motions were recorded in sites with shear wave velocities between 180–750 m/s, the magnitude of earthquakes was greater than 5.5, and the source-to-site distance was less than 100 km. The ground motion set that was selected by Baker contained 267 pairs of horizontal records. In this study, 23 pairs from the 267 pairs of records, which were excluded from the NGA database, were omitted (these 23 pairs include records from the Taiwan SMART1(40) and SMART1(45) earthquakes). In addition, records with a minimum usable frequency greater than 0.2 Hz were also omitted. Thus, 350 ground motion records from the ground motion set used by Baker (2005) and the ground motion set used by Haselton and Deierlein (2008) with a minimum usable frequency ≤ 0.2 Hz were selected. The ground motion records come from various active shallow crustal tectonic regions throughout the world (e.g., California, Turkey, Italy, Japan, Taiwan, and Iran), and are related to earthquakes with magnitudes of 5.5–7.6.

Having a GMPE for an IM, the epsilon for that IM ($\varepsilon_{\mathrm{IM}}$) can be calculated as follows:

$$\varepsilon_{\mathrm{IM}} = \frac{\ln \mathrm{IM} - \mu_{\ln \mathrm{IM}}}{\sigma_{\ln \mathrm{IM}}} \tag{14}$$

Table 8 Parameters in Eq. (13) defining the piece-wise variation of the correlation between $\ln S_a(T)$ and ln DSI ($\rho_{\ln Sa(T), \ln \mathrm{DSI}}$)

n	e_n	a_n	b_n	c_n	d_n
0	0.01	-	-	-	-
1	0.15	0.39	0.265	0.04	1.8
2	3.40	0.19	1.200	1.20	0.6
3	10.0	0.98	0.820	6.10	3.0

where $\ln$ IM is the natural logarithm of the IM observed in a particular ground motion; $\mu_{\ln \mathrm{IM}}$ and $\sigma_{\ln \mathrm{IM}}$ are the predicted mean and standard deviation of $\ln$ IM, respectively. In other words, $\varepsilon_{\mathrm{IM}}$ is the number of standard deviations by which an observed $\ln$ IM differs from the predicted mean ($\mu_{\ln \mathrm{IM}}$). As pointed out by Bradley (2011b and 2012), due to the linear relationship between $\ln$ IM and $\varepsilon_{\mathrm{IM}}$, the correlation between the logarithms of two IMs for a given earthquake rupture is equal to the correlation between their epsilons. Hence, to obtain the correlation between $\ln S_a(T)$ and $\ln (S_a(T)/\mathrm{DSI})$, $\rho_{\ln Sa(T), \ln (Sa(T)/\mathrm{DSI})}$, the correlation between ε_{Sa} and $\varepsilon_{Sa/\mathrm{DSI}}$, $\rho_{\varepsilon_{Sa}, \varepsilon_{Sa/\mathrm{DSI}}}$, was calculated. The Campbell and Bozorgnia (2007) GMPE was applied for the calculation of ε_{Sa} values. Furthermore, the model presented in Section 8.1 was used to calculate $\varepsilon_{Sa/\mathrm{DSI}}$ values. To use this model, the Campbell and Bozorgnia GMPE and the method proposed by Bradley (2011a) were applied for obtaining the means and standard deviations required in Eqs. (11) and (12). Figure 10 presents the correlation coefficients between ε_{Sa} and $\varepsilon_{Sa/\mathrm{DSI}}$ in different periods, obtained by using the selected ground motion set (which contains 350 records). By applying a third-order polynomial regression on the correlation coefficients in different periods, an equation was proposed to obtain $\rho_{\ln Sa(T), \ln (Sa(T)/\mathrm{DSI})}$ as a function of period as follows:

$$\rho_{\ln Sa(T), \ln (Sa(T)/\mathrm{DSI})} = \rho_{\varepsilon_{Sa}, \varepsilon_{Sa/\mathrm{DSI}}} = aT^3 + bT^2 + cT + d$$
$$a = 0.008,\ b = -0.021,\ c = -0.093,\ d = 0.614 \tag{15}$$

After calculating the $\varepsilon_{Sa/\mathrm{DSI}}$ values in different periods for the 350 ground motion records by using the model presented in Section 8.1, the Kolmogorov-Smirnov (KS) test (Hogg and Ledolter, 1987) was applied to examine the distribution of $\varepsilon_{Sa/\mathrm{DSI}}$. The results of the KS tests confirmed the normal distribution of $\varepsilon_{Sa/\mathrm{DSI}}$ values in different periods. Figure 11 illustrates the empirical and normal CDFs of $\varepsilon_{Sa/\mathrm{DSI}}$ in periods of 1.0 and 1.5 s. As shown in this figure, the empirical distributions of $\varepsilon_{Sa/\mathrm{DSI}}$ in both periods are well approximated by the normal distribution. Therefore, the assumption of a lognormal distribution for $S_a(T_1)$/DSI is reasonable.

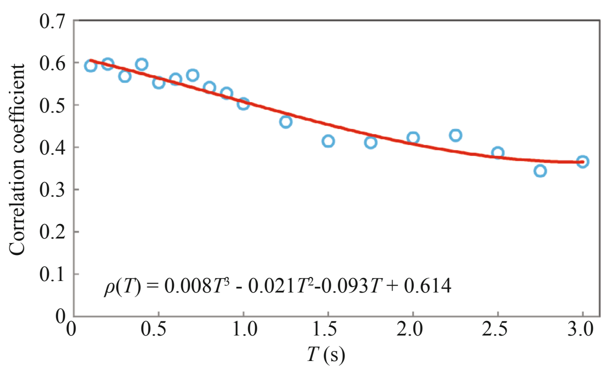

Fig. 10 Correlation coefficients between ε_{Sa} and $\varepsilon_{Sa/\mathrm{DSI}}$ in different periods

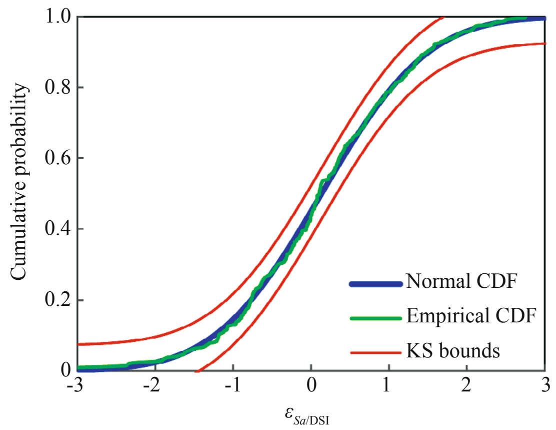

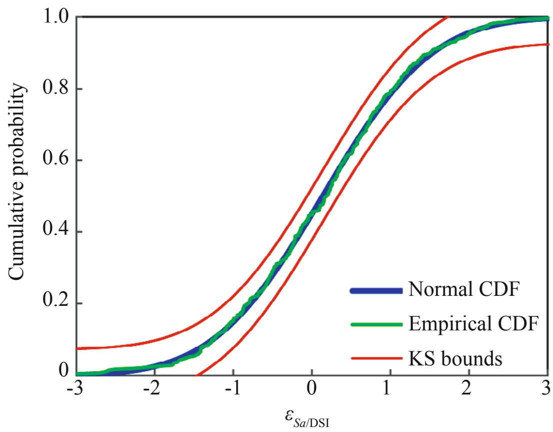

Fig. 11 Comparison between the empirical and normal CDFs of $\varepsilon_{Sa/\mathrm{DSI}}$ in periods of: (a) T = 1.0 s and (b) T = 1.5 s

9 Discussion and future work

The results of this study show that using the ratio of two scalar IMs as the second component of a vector-valued IM may lead to great efficiency for predicting the collapse capacity of structures. Among the ratios of scalar IMs considered as IM_2 parameters, some have acceptable correlation with the structural collapse capacity; nevertheless, because they do not satisfy the sufficiency criteria for some or all of the structures, they cannot be considered as the second component of an optimal vector-valued IM. For instance, $S_a(T_1)$/PGD, which has relatively high correlation with the structural collapse capacity, does not satisfy the sufficiency criteria for the low-rise structures. It should be noted that the vector ($S_a(T_1)$, $S_a(T_1)$/PGD) can be used for reliable seismic collapse assessment of mid- to high-rise structures.

Procedures for selecting and scaling ground motion records for a specific hazard level have been the subject of much research in recent years (e.g., Iervolino and Manfredi, 2008; Kalkan and Chopra, 2010). As an alternative to the direct use of a vector-valued IM, ground motion records can be selected based on one component of the vector-valued IM, and then the seismic assessment can be performed by using the other component (i.e., IM_1). For example, as mentioned by Baker (2005), instead of using ($S_a(T_1)$, ε_{Sa}) as a vector-valued IM in the analyses, one can select ground motion records based on the target ε_{Sa} and then perform the analyses by using $S_a(T_1)$ as a scalar IM. The target ε_{Sa} for a specific seismic hazard level is obtained from seismic hazard disaggregation (McGuire, 1995; Bazzurro and Cornell, 1999). Similarly, instead of using ($S_a(T_1)$, $S_a(T_1)$/DSI) as a vector-valued IM, ground motion selection for a specific seismic hazard level can be performed based on the target value of $S_a(T_1)$/DSI. To obtain the target $S_a(T_1)$/DSI, the GMPE for $S_a(T)$/DSI, the correlation between ln $S_a(T)$ and ln ($S_a(T)$/DSI) proposed in Section 8, and the target ε_{Sa} are needed. Then, the method used by Bradley (2010b) can be employed to determine the target $S_a(T_1)$/DSI. After the selection of records based on the target $S_a(T_1)$/DSI, seismic analyses can be performed by using $S_a(T_1)$ as a scalar IM.

It is worth noting that the technical literature includes some scalar and vector-valued IMs with variable parameters, which can be optimized based on the structural characteristics (e.g., the IMs used by Vamvatsikos and Cornell, 2005). Therefore, optimizing these IMs and performing a comprehensive comparison between the IM proposed in this study and the optimized scalar and vector-valued IMs can be an interesting open field for future studies.

10 Conclusions

In this study, different IMs were considered for seismic collapse assessment of low- to high-rise structures. The considered IMs include $S_a(T_1)$ as a scalar IM and twelve vector-valued IMs consisting of two components. After investigating the desirable features of an optimal IM, the vector ($S_a(T_1)$, $S_a(T_1)$/DSI) was proposed as an optimal vector-valued IM for seismic collapse assessment of structures.

The results show that the vector ($S_a(T_1)$, $S_a(T_1)$/DSI) is more efficient than the other IMs for collapse capacity prediction of the structures. As an example, in the case of an 8-story structure, the use of this vector-valued IM was found to cause more than 50% reduction in the estimated dispersion of collapse capacity in comparison with the use of $S_a(T_1)$ as a scalar IM. Thus, by using this vector-valued IM, the number of required analyses can be reduced more than four times while the standard error remains the same. Further, the results show that $S_a(T_1)$ as a scalar IM is not sufficient with respect to magnitude and scale factor for collapse capacity prediction. This insufficiency can be improved by adding a proper parameter as the second component to $S_a(T_1)$ and developing a vector-valued IM. Among the second components of the considered vector-valued IMs, the use of the parameter $S_a(T_1)$/DSI was found to lead to significant sufficiency with respect to magnitude for collapse capacity prediction of the structures. Due to the sufficiency of $S_a(T_1)$ with respect to source-to-site distance, the proposed vector-valued IM containing $S_a(T_1)$ as the first component is also sufficient with respect to source-to-site distance. Furthermore, the new IM satisfies the scaling robustness criterion (sufficiency with respect to scale factor) for collapse capacity prediction of the structures. In fact, the considerable efficiency and sufficiency of the proposed IM increases the reliability of seismic collapse assessment by reducing the dispersion and bias in the prediction of structural collapse capacity.

To satisfy the predictability criterion for ($S_a(T_1)$, $S_a(T_1)$/DSI), a GMPE was determined for $S_a(T_1)$/DSI by applying the existing GMPEs. Furthermore, an empirical equation was proposed for obtaining the correlation between $\ln S_a(T)$ and $\ln (S_a(T)/\text{DSI})$ as a function of period.

Acknowledgement

The authors express their sincere gratitude to Dr. Vamvatsikos for his valuable comments. The authors also acknowledge Dr. Haselton for providing the structural models on his website.

References

Ang AHS and Tang WH (1975), *Probability Concepts in Engineering Planning and Design Volume. Volume I—Basic Principles*, Wiley, Inc., New York.

Arias A, (1970), "A Measure of Earthquake Intensity," *Seismic Design for Nuclear Power Plants, R. J. Hansen* (*ed.*), The MIT Press, Cambridge, MA, 438–483.

ASCE 41–06 (2007), "Seismic Rehabilitation of Existing Buildings," *ASCE-SEI Standard 41–06*, American Society of Civil Engineers, Reston, VA.

Baker JW (2005), "Vector-valued Ground Motion Intensity Measures for Probabilistic Seismic Demand Analysis," *Ph.D. Dissertation*, Department of Civil and Environmental Engineering, Stanford University, Stanford, CA.

Baker JW and Cornell CA (2005), "A Vector-valued Ground Motion Intensity Measure Consisting of Spectral Acceleration and Epsilon," *Earthquake Engineering and Structural Dynamics*, **34**(10): 1193–1217.

Baker JW and Cornell CA (2008a), "Vector-valued Intensity Measures for Pulse-like Near-fault Ground Motions," *Engineering Structures*, **30**(4): 1048–1057.

Baker JW and Cornell CA (2008b), "Vector-valued Intensity Measures Incorporating Spectral Shape for Prediction of Structural Response," *Journal of Earthquake Engineering*, **12**(4): 534–554.

Bazzurro P and Cornell CA (1999), "On Disaggregation of Seismic Hazard," *Bulletin of the Seismological Society of America*, **89**(2): 501–520.

Bazzurro P and Cornell CA (2002), "Vector-valued Probabilistic Seismic Hazard Analysis," *7th U.S. National Conference on Earthquake Engineering*, Boston, MA.

Bojórquez E and Iervolino I (2010), "A Spectral Shape-based Scalar Ground Motion Intensity Measure for Maximum and Cumulative Structural Demands," *Proceedings of 14th European Conference on Earthquake Engineering*, Ohrid, Macedonia.

Bojórquez E and Iervolino I (2011), "Spectral Shape Proxies and Nonlinear Structural Response," *Soil Dynamics and Earthquake Engineering*, **31**(7): 996–1008.

Bojórquez E, Iervolino I, Reyes-Salazar A and Ruiz SE (2012), "Comparing Vector-valued Intensity Measures for Fragility Analysis of Steel Frames in the Case of Narrow-band Ground Motions," *Engineering Structures*, **45**: 472–480.

Bradley BA (2010a), "Site-specific and Spatially Distributed Ground-motion Prediction of Acceleration Spectrum Intensity," *Bulletin of the Seismological Society of America*, **100**(2): 277–285.

Bradley BA (2010b), "A Generalized Conditional Intensity Measure Approach and Holistic Ground-motion Selection," *Earthquake Engineering and Structural Dynamics*, **39**(12): 1321–1342.

Bradley BA (2011a), "Empirical Equations for the Prediction of Displacement Spectrum Intensity and Its Correlation with Other Intensity Measures," *Soil Dynamics and Earthquake Engineering*, **31**(8): 1182–1191.

Bradley BA (2011b), "Empirical Correlation of PGA, Spectral Accelerations and Spectrum Intensities from Active Shallow Crustal Earthquakes," *Earthquake Engineering and Structural Dynamics*, **40**(15): 1707–1721.

Bradley BA (2012), "Empirical Correlations between Peak Ground Velocity and Spectrum-Based Intensity Measures," Earthquake Spectra, **28**(1): 17–35.

Bradley BA, Cubrinovski M, Dhakal RP and MacRae GA (2009a), "Intensity Measures for the Seismic Response of Pile Foundations," *Soil Dynamics and Earthquake Engineering*, **29**(6): 1046–1058.

Bradley BA, Cubrinovski M, MacRae GA and Dhakal RP (2009b), "Ground-motion Prediction Equation for SI Based on Spectral Acceleration Equations," *Bulletin of the Seismological Society of America*, **99**(1): 277–285.

Bradley BA, Dhakal RP, MacRae GA and Cubrinovski M (2010), "Prediction of Spatially Distributed Seismic Demands in Specific Structures: Ground Motion and Structural Response," *Earthquake Engineering and*

Structural Dynamics, **39**(5): 501–520.

Campbell KW and Bozorgnia Y (2007), "Campbell–Bozorgnia NGA Ground Motion Relations for the Geometric Mean Horizontal Component of Peak and Spectral Ground Motion Parameters," *PEER Report 2007/02*, Pacific Engineering Research Center, University of California, Berkeley, CA.

Campbell KW and Bozorgnia Y (2012), "A Comparison of Ground Motion Prediction Equations for Arias Intensity and Cumulative Absolute Velocity Developed Using a Consistent Database and Functional Form," *Earthquake Spectra,* **28**(3): 931–941.

Eads L, Miranda E, Krawinkler H and Lignos DG (2013), "An Efficient Method for Estimating the Collapse Risk of Structures in Seismic Regions," *Earthquake Engineering and Structural Dynamics*, **42**(1): 25–41.

Gehl P, Seyedi DM and Douglas J (2013), "Vector-valued Fragility Functions for Seismic Risk Evaluation," *Bulletin of Earthquake Engineering*, **11**(2): 365–384.

Goulet CA, Haselton CB, Mitrani-Reiser J, Beck JL, Deierlein GG, Porter KA and Stewart JP (2007), "Evaluation of the Seismic Performance of a Code-conforming Reinforced-concrete Frame Building–from Seismic Hazard to Collapse Safety and Economic Losses," *Earthquake Engineering and Structural Dynamics*, **36**(13): 1973–1997.

Haselton CB and Baker JW (2006), "Ground Motion Intensity Measures for Collapse Capacity Prediction: Choice of Optimal Spectral Period and Effect of Spectral Shape," *Proceedings of 8th National Conferrance on Earthquake Engineering*, Earthquake Engineering Research Institute, Oakland, CA.

Haselton CB, Baker JW, Liel AB and Deierlein GG (2011), "Accounting for Ground Motion Spectral Shape Characteristics in Structural Collapse Assessment through an Adjustment for Epsilon," *Journal of Structural Engineering*, *ASCE*, **137**(3): 332–344.

Haselton CB and Deierlein GG (2008), "Assessing Seismic Collapse Safety of Modern Reinforced Concrete Moment-frame Buildings," *PEER Report 2007/08*, Pacific Earthquake Engineering Research Center, University of California, Berkeley, CA.

Haselton CB, Liel AB, Taylor Lange S and Deierlein GG (2008), "Beam-column Element Model Calibrated for Predicting Flexural Response Leading to Global Collapse of RC Frame Buildings, " *PEER Report 2007/03*, Pacific Earthquake Engineering Research Center, University of California, Berkeley, CA.

Hogg RV and Ledolter J (1987), *Engineering Statistics*, MacMillan, New York.

Housner GW (1952), "Spectrum Intensities of Strong-motion Earthquakes," *Symposium on Earthquakes and Blast Effects on Structures*, Los Angeles, California.

Housner GW (1963), "The Behavior of Inverted Pendulum Structures during Earthquakes," *Bulletin of the Seismological Society of America*, **53**(2), 403–417.

Iervolino I and Manfredi G, (2008), *A Review of Ground Motion Record Selection Strategies for Dynamic Structural Analysis, Modern Testing Techniques for Structural Systems*, Bursi OS and Wagg D (Editors), CISM International Centre for Mechanical Sciences, 502, 131–163.

Kaklamanos J, Baise GL and Boore DM (2011), "Estimating Unknown Input Parameters when Implementing the NGA Ground-motion Prediction Equations in Engineering Practice," *Earthquake Spectra*, **27**(4): 1219–1235.

Kalkan E and Chopra AK (2010), "Practical Guidelines to Select and Scale Earthquake Records for Nonlinear Response History Analysis of Structures," *USGS Open File Report 2010-1068*.

Kutner MH, Nachtsheim CJ, Neter J and Li W (2005), *Applied Linear Statistical Models*, McGraw-hill, Boston.

Luco N and Cornell CA (2007), "Structure-specific Scalar Intensity Measures for Near-source and Ordinary Earthquake Ground Motions," *Earthquake Spectra*, **23**(2): 357–392.

McGuire RK (1995), "Probabilistic Seismic Hazard Analysis and Design Earthquakes: Closing the Loop," *Bulletin of the Seismological Society of America*, **85**(5): 1275–1284.

Open System for Earthquake Engineering Simulation (OpenSees) (2006), Pacific Earthquake Engineering Research Center, University of California, Berkeley, http://opensees.berkeley.edu.

Pacific Earthquake Engineering Research Center (PEER) (2008), *PEER Next Generation Attenuation* (*NGA*) *Database*. http://peer.berkeley.edu/nga.

Rajeev P, Franchin P and Pinto PE (2008), "Increased Accuracy of Vector-IM-Based Seismic Risk Assessment?" *Journal of Earthquake Engineering*, **12**(S1): 111–124.

Seyedi DM, Gehl P, Douglas J, Davenne L, Mezher N and Ghavamian S (2010), "Development of Seismic Fragility Surfaces for Reinforced Concrete Buildings by Means of Nonlinear Time-history Analysis," *Earthquake Engineering and Structural Dynamics*, **39**(1): 91–108.

Sezen H, Elwood KJ, Whittaker AS, Mosalam KM, Wallace JW and Stanton JF (2000), "Structural Engineering Reconnaissance of the August 17, 1999, Kocaeli (Izmit), Turkey, Earthquake," *PEER Report 2000/09*, Pacific Earthquake Engineering Research Center, University of California, Berkeley, CA.

Tang B, Lu X, Ye L and Shi W (2011), "Evaluation of Collapse Resistance of RC Frame Structures for Chinese Schools in Seismic Design Categories B and C," *Earthquake Engineering and Engineering Vibration*, **10**(3): 369–377.

Tothong P and Cornell CA (2008), "Structural Performance Assessment under Near-source Pulse-like Ground Motions Using Advanced Ground Motion Intensity Measures," *Earthquake Engineering and Structural Dynamics*, **37**(7): 1013–1037.

Tothong P and Luco N (2007), "Probabilistic Seismic Demand Analysis Using Advanced Ground Motion Intensity Measures," *Earthquake Engineering and Structural Dynamics*, **36**(13): 1837–1860.

Tsantaki S and Adam C (2013), "Collapse Capacity Spectra Based on an Improved Intensity Measure," *Proceedings of 4th ECCOMAS Thematic Conference on Computational Methods in Structural Dynamics and Earthquake Engineering*, (*COMPDYN 2013*), Kos Island, Greece.

Vamvatsikos D and Cornell CA (2002), "Incremental Dynamic Analysis," *Earthquake Engineering and Structural Dynamics*, **31**(3): 491–514.

Vamvatsikos D and Cornell CA (2005), "Developing Efficient Scalar and Vector Intensity Measures for IDA Capacity Estimation by Incorporating Elastic Spectral Shape Information," *Earthquake Engineering and Structural Dynamics*, **34**(13): 1573–1600.

Villaverde R (2007), "Methods to Assess the Seismic Collapse Capacity of Building Structures: State of the Art," *Journal of Structural Engineering*, ASCE, **133**(1): 57–66.

Von Thun JL, Roehm LH, Scott GA and Wilson JA (1988), "Earthquake Ground Motions for Design and Analysis of Dams," *Proceedings of the Earthquake Engineering and Soil Dynamics II-Recent Advances in Ground Motion Evaluation, Geotechnical Special Publication*, ASCE, New York, 463–481.

Wang Y (2008), "Lessons Learned from the "5.12" Wenchuan Earthquake: Evaluation of Earthquake Performance Objectives and the Importance of Seismic Conceptual Design Principles," *Earthquake Engineering and Engineering Vibration*, **7**(3): 255–262.

Zareian F (2006), "Simplified Performance-based Earthquake Engineering," *Ph.D. Dissertation*, Department of Civil and Environmental Engineering, Stanford University, Stanford, CA.